# TUDelft

Delft University of Technology

## Nitrous oxide emission in a University of Cape Town membrane bioreactor
## The effect of carbon to nitrogen ratio

Mannina, Giorgio; Capodici, Marco; Cosenza, Alida; Di Trapani, Daniele; van Loosdrecht, Mark C.M.

**Important note**
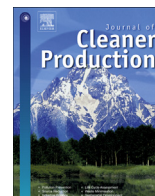To cite this publication, please use the final published version (if applicable).
Please check the document version above.

# Nitrous oxide emission in a University of Cape Town membrane bioreactor: The effect of carbon to nitrogen ratio

Giorgio Mannina [a], Marco Capodici [a], Alida Cosenza [a, *], Daniele Di Trapani [a], Mark C.M. van Loosdrecht [b]

[a] Dipartimento di Ingegneria Civile, Ambientale, Aerospaziale, dei Materiali, Università di Palermo, Viale delle Scienze, Ed. 8, 90100, Palermo, Italy
[b] Department of Biotechnology, Delft University of Technology, Julianalaan 67, 2628 BC, Delft, Netherlands

**A B S T R A C T**

The effect of the carbon-to-nitrogen (C/N) ratio in the influent on the nitrous oxide ($N_2O$) emission from a University of Cape Town Membrane BioReactor pilot plant was investigated. The membrane was located in a separate tank to single out the production of $N_2O$ due to the biological processes from $N_2O$ stripping as a result of the extra aeration needed for the mitigation of membrane fouling. The experimental campaign was divided into two phases, each characterized by a different C/N ratio (namely, 10 and 5 mgCOD/mgTN, Phase I and Phase II, respectively). The decrease of the C/N ratio promoted the increase of $N_2O$ emissions in both gaseous and dissolved phases, mainly due to a decreased nitrification/denitrification capacity of the system. The highest $N_2O$ concentration in the dissolved phase was found in the permeate. This result suggests that the dissolved $N_2O$ in the permeate stream discharged from a MBR cannot be neglected. The total $N_2O$ emission was approximately of 0.01% and 0.1% of the total influent nitrogen load for the Phase I and Phase II, respectively. The findings suggest that the C/N ratio represents an indirect cause of $N_2O$ emission; the low C/N value (Phase II) led to the increase of pH and free ammonia causing a stress effect on the growth of nitrifying species increasing the $N_2O$ emission.

© 2017 Elsevier Ltd. All rights reserved.

## 1. Introduction

Nitrous oxide ($N_2O$) is a greenhouse gas (GHG) that has a great climate change potential. The global warming potential (GWP) of $N_2O$ is 298 times higher than carbon dioxide ($CO_2$), moreover it has the capability to react with stratospheric ozone causing ozone layer depletion (IPCC, 2007). Therefore, the reduction of anthropogenic $N_2O$ emissions is becoming an imperative requirement for governments worldwide. As a result, $N_2O$ emissions from wastewater treatment has received increasing attention in recent years (Mannina et al., 2016a). $N_2O$ can be produced and directly emitted from wastewater treatment plants (WWTPs). Therefore, the $N_2O$ emission has to be taken into account to reduce the WWTP environmental impacts (Papa et al., 2016; Frison et al., 2015). Specifically, $N_2O$ generation mainly occurs in biological nitrogen removal (BNR) via nitrification and denitrification processes (Kampschreur et al., 2009).

Previous studies showed that factors affecting the nitrification and denitrification efficiency (i.e., dissolved oxygen, carbon to nitrogen (C/N) ratio, sludge retention time, temperature, nitrite etc.) are the major causes for $N_2O$ emissions from WWTPs (Quan et al., 2012; Wu et al., 2014). Regarding the C/N ratio, Stenström et al. (2014) found that the low C/N ratio ($2.3 \pm 0.2$) coupled with the high nitrite ($NO_2$-N) (>40 mg L$^{-1}$) concentration promote the $N_2O$ formation during the denitrification. On the other hand, Quan et al. (2012) found that for aerobic granular sludge, $N_2O$ emissions during denitrification increased with the decrease of the C/N ratio. Li et al. (2013) found that high organic shock loads (from 200 to 350 or 500 mg L$^{-1}$) increase the $N_2O$ production from denitrifiers phosphorus-accumulating organisms (DPAOs) and decrease the P removal efficiency. Therefore, Li et al. (2013) suggested the use of the low influent C/N ratio (1 or 2) in order to reduce the DPAOs contribution of $N_2O$ formation; *viceversa*, in case of high C/N (equal or higher than 7), the adoption of continuous nitrate addition is suggested. Wu et al. (2014) for a sequential batch reactor system found that with increasing C/N ratios (from 1 to 4) the denitrification rate increased with a consequent decrease of $N_2O$ emissions (from 80 mg L$^{-1}$ to 8 mg L$^{-1}$).

\* Corresponding author.
  *E-mail address:* alida.cosenza@unipa.it (A. Cosenza).

Regarding $N_2O$ emissions from MBRs, only few studies have been carried out so far (among others, Mannina et al., 2016c; Nuansawan et al., 2016). Mannina et al. (2016c) for a sequential batch MBR pilot plant found a worsening of the nitrification efficiency with the increase of inlet salinity concentration and the increase of $N_2O$ emissions. Nuansawan et al. (2016) investigated a two-stage (anaerobic/aerobic) MBR treating solid waste leachate; they found the increase of $N_2O$ emission with the decrease (till to 5 days) of the hydraulic retention time (HRT). However, the transferability of the findings derived for conventional activated sludge systems (CASs) is limited. Indeed, MBRs are characterized by some specific peculiarities (biomass selection; absence of secondary clarifier which can contribute in $N_2O$ production; intensive aeration for fouling mitigation in membrane compartment which can promote $N_2O$ stripping; etc.) which hamper a direct transferability of the results derived for CAS systems. Further, to the authors' knowledge no studies have been reported on the effects of the C/N ratio on the $N_2O$ from a BNR-MBR pilot plant. Further, previous studies have been focused on industrial wastewaters (namely, saline or leachate) (Mannina et al., 2016c; Nuansawan et al., 2016) and are based almost on batch experiments with scarce analyses on continuous-fed dynamic plants (Quan et al., 2012; Stenström et al., 2014; Wu et al., 2014; Li et al., 2013). However, as recently demonstrated by Sperandio et al. (2016) long terms analysis is relevant for taking into account the evolution of the biomass properties over the time and their influence in $N_2O$ formation. .

The authors have already conducted a study on the performances of the University Cape Town membrane bioreactor (UCT-MBR) pilot plant (i.e., Mannina et al., 2016b). This paper is the continuation of that work, and focuses on the quantification of $N_2O$ emissions. In particular, the paper is aimed at exploring the impact of the C/N ratio on $N_2O$ emissions in a continuously operated plant, capturing the overall $N_2O$ emission from an MBR system.

## 2. Material and methods

### 2.1. The UCT-MBR pilot plant

A UCT-MBR pilot plant (Fig. 1) was monitored for 100 days (Mannina et al., 2016b). The pilot plant consisted of an anaerobic (volume 62 L), anoxic (volume 102 L) and aerobic (volume 211 L) tank according to the UCT scheme. The solid-liquid separation phase was achieved by means of an ultrafiltration hollow fibre membrane module (PURON® Triple bundle Demo Module). The

membrane module (nominal pore size 0.03 μm, membrane area 1.4 m²) was located inside a dedicated aerated tank (referred to as the MBR tank, with a 36 L volume). During both the experimental periods, the membrane was operated by applying a specific aeration demand based on membrane ($SAD_m$) of 0.41 m³ m⁻² h⁻¹. While, a value of 24 m³ m⁻³ for the specific aeration demand based on permeate volume ($SAD_p$) was adopted. The values of $SAD_m$ and $SAD_p$ were evaluated according to Judd and Judd (2010) and are in agreements with the manufacture's operation suggestion. An oxygen depletion reactor (ODR) allowed oxygen removal in the mixed liquor recycled from the MBR tank to the anoxic tank ($Q_{RAS}$). The aeration flow rate was on average equal to 19.85 L min⁻¹ and 9.53 L min⁻¹ for aerobic and MBR tank, respectively. The membrane was periodically backwashed (every 9 min for a period of 1 min) by pumping a volume of permeate back through the membrane fibres from the Clean In Place (CIP) tank ($Q_{BW}$ represents the backwashing flow rate); an instantaneous permeate flux of 21 L m⁻² h⁻¹ was used ($Q_{OUT,IST}$) (the membrane critical flux, indicated by manufactures, is of 32 L m⁻² h⁻¹). The influent flow rate was set equal to 20 L h⁻¹ ($Q_{IN}$). During the pilot plant operation, a 20 L h⁻¹ flow ($Q_{R1}$) was continuously pumped from the anoxic to the anaerobic tank. Furthermore, 100 L h⁻¹ ($Q_{R2}$) of mixed liquor was pumped from the aerobic to the MBR tank. A net permeate flow rate of 20 L h⁻¹ was extracted ($Q_{OUT}$) through the membrane. Therefore, the recycled activated sludge ($Q_{RAS}$) from the MBR to the anoxic tank through the ODR tank was equal to 80 L h⁻¹. An average DO concentration of 3.2 mg L⁻¹ and 4.2 mg L⁻¹ was maintained during both the experimental periods inside the aerobic and MBR tanks, respectively. The anaerobic, anoxic, aerobic and MBR tanks were equipped with specific covers that guaranteed gas accumulation in the headspace to perform the gas sampling. During the pilot plant operation, a very low waste sludge (around the 0.8% of the influent rate) was extracted from the bottom valve of the aerobic reactor.

### 2.2. Experimental campaign and influent wastewater features

The experimental campaign was divided into two phases, each characterized by a different C/N ratio: Phase I, C/N = 10 mgCOD/mgTN; Phase II, C/N = 5 mgCOD/mgTN.

The UCT-MBR pilot plant was fed with real wastewater collected at the University campus and mixed with a synthetic mixture of sodium acetate ($CH_3COONa$) (35%), glycerol ($C_3H_8O_3$) (65%), dipotassium hydrogen phosphate ($K_2HPO_4$) and ammonium chloride ($NH_4Cl$). In Table 1 summarizes the main influent and operational



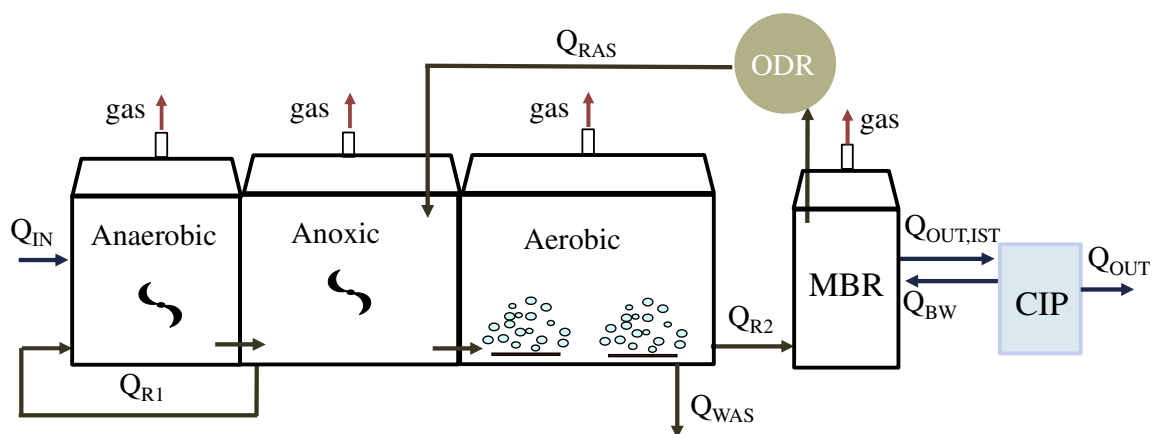**Fig. 1.** Layout of the UCT-MBR pilot plant. Where: $Q_{in}$ = influent wastewater; $Q_{R1}$ = mixed liquor recycled from the anoxic to the anaerobic tank; $Q_{R2}$ = mixed liquor recycled from the aerobic to the MBR tank; $Q_{RAS}$ = Recycled sludge from the MBR to the anoxic tank; $Q_{OUT}$ = effluent permeate flow rate; ODR = Oxygen Depletion Reactor; $Q_{OUT,IST}$ = suction flow rate $Q_{BW}$ = backwashing flow rate.

**Table 1**
Average features and standard deviation (SD) of the inlet wastewater and operation conditions during the Phases I and II (in brackets the percentage of synthetic wastewater).

| Parameter | Units | Phase I | | Phase II | |
|---|---|---|---|---|---|
| | | Average value | SD | | SD |
| COD | [mg L$^{-1}$] | 502 (71%) | ±145 | 411 (58%) | ±57 |
| BOD | [mg L$^{-1}$] | 152 (73%) | ±15 | 162 (61%) | ±22 |
| Total nitrogen (TN) | [mg L$^{-1}$] | 52.6 (0.0%) | ±13.2 | 99.2 (51.68%) | ±29 |
| NH$_4$-N | [mg L$^{-1}$] | 48.1 (0.0%) | ±9.8 | 92.92 (47.7%) | ±31 |
| Total phosphorus (TP) | [mg L$^{-1}$] | 4.2 (10.94%) | ±0.5 | 5.4 (11.43%) | ±1.2 |
| Permeate Flux | [L m$^{-2}$ h$^{-1}$] | 21 | ±2 | 21 | ±2 |
| Flow rate | [L h$^{-1}$] | 20 | ±1.5 | 20 | ±0.8 |
| COD/N | [mgCOD/mgTN] | 10 | − | 5 | − |
| HRT | [h] | 20 | − | 20 | − |
| Experimental period | [d] | 21−61 | − | 62−99 | − |

features of both experimental phases.

During the pilot plant operation, the influent wastewater, the mixed liquor inside the anaerobic, anoxic, aerobic and MBR tanks, and the effluent permeate were sampled and analysed for TSS, volatile suspended solids (VSS), total chemical oxygen demand (COD$_{TOT}$), supernatant COD (COD$_{SUP}$), ammonium nitrogen (NH$_4$-N), nitrite nitrogen (NO$_2$-N), nitrate nitrogen (NO$_3$-N), total nitrogen (TN), phosphate (PO$_4$-P), and total phosphorus (TP), Biochemical Oxygen Demand (BOD). All analyses were performed according to the Standard Methods (APHA, 2005). Furthermore, pH, DO and temperature were also monitored in each tank using a multiparameter probe. Furthermore, as detailed below, nitrous oxide (N$_2$O) dissolved and in the gas samples was analysed. N$_2$O concentration was measured by using a Gas Chromatograph (Thermo Scientific™ TRACE GC) equipped with an Electron Capture Detector. Moreover, respirometric batch tests aimed at evaluating biokinetic parameters, ammonium utilization rate (AUR) and nitrate utilization rate (NUR) batch tests were performed as detailed in Mannina et al. (2016b). Further details on the experimental campaign can be found in Mannina et al. (2016b).

### 2.3. Pilot plant removal performances

The UCT-MBR pilot plant performance was evaluated in terms of COD removal, nitrification/denitrification efficiency, total nitrogen removal and phosphorus removal. To discriminate between the removal effect of the biological processes and the filtration of the membrane, two different removal efficiencies for the COD were calculated (Mannina et al., 2016b): the biological removal efficiency ($\eta_{BIO}$) and the total removal efficiency ($\eta_{TOT}$). The former was calculated as the difference between the total COD (COD$_{TOT}$) value in the influent and the COD measured in the supernatant of mixed liquor samples (filtered at 0.45 μm) withdrawn from the MBR tank (COD$_{SUP}$). Conversely, the total COD removal efficiency (also including the effect of the removal effect of the membrane filtration) was assessed as the difference between the COD$_{TOT}$ in the influent and in the permeate.

Nitrification ($\eta_{nit}$), denitrification ($\eta_{denit}$) and nitrogen ($\eta N_{total}$) removal efficiencies were evaluated according to literature (Mannina et al., 2016a,b and Wagner et al., 2015).

### 2.4. Gas sampling

The liquid and gaseous samples were withdrawn from the anaerobic, anoxic, aerobic and MBR tanks and analysed to determine the N$_2$O-N concentration. Furthermore, the N$_2$O-N fluxes (gN$_2$O-N m$^{-2}$ h$^{-1}$) from all the compartments were quantified by measuring the gas flow rates, Q$_{gas}$ (L min$^{-1}$), as outlined in sections 2.4.1 and 2.4.4.

#### 2.4.1. Gas flow rate measurement

Q$_{gas}$ was indirectly evaluated according to Equation [1]:

$$Q_{gas} = v_{gas} \cdot A \tag{1}$$

where A represents the outlet section (m$^2$) and v$_{gas}$ (m s$^{-1}$) is the gas velocity, measured by using the TMA-21HW - Hot Wire anemometer. During the flow rate measurements in the non-aerated compartments, a sweep air flow rate (Q$_{Sweep}$) was supplied inside the reactor to promote gas mixing and facilitate gas sampling at low gas flow rate conditions (Chandran et al., 2011). Thus, the gas flow rate emitted from the anoxic tank was evaluated according to Equation [2].

$$Q_{gas} = v_{gas} \cdot A - Q_{Sweep} \tag{2}$$

#### 2.4.2. Gas phase sampling

Gas samples were withdrawn by means of commercial syringes and transferred into glass vials (e.g., LABCO Exetainer, 738 model) where the vacuum was previously created.

To guarantee the atmospheric pressure inside the vials, the ratio between the volume of the gas sample (inserted inside the vial) and the volume of the vial was no less than 1.25 (e.g., 15 mL of sample in a 12 mL vial).

Three replicates were performed for each grab sample. The N$_2$O-N concentration was then calculated as the average value among the 3 replicates.

#### 2.4.3. Dissolved gas sampling

Dissolved gas sampling was conducted on the basis of the head space gas method derived from Kimochi et al. (1998). In detail, 70 mL of supernatant (after 5 min of centrifugation at 8000 rpm) were sealed into 125 mL glass bottles. To prevent any biological reaction, 1 mL of 2N H$_2$SO$_4$ was added. After 24 h of gentle stirring, the bottles were left for 1 h without moving. Thereafter, the gas accumulated in the headspace of the bottles was collected similarly to the gas sampling procedure.

Finally, by applying Henry's Law, the dissolved gas concentration at equilibrium with the headspace gas was calculated. In this case, a lower sampling frequency was used (1 sample per hour). Further details can be derived from literature (see Mannina et al., 2016d).

#### 2.4.4. Gas flux quantification

The i-th gas flux (F$_i$) emitted from the j-th tank was quantified according to Equation [3] derived from Yan et al. (2014).

$$F_i = \rho_i \cdot C_i \frac{Q_{gas,j}}{A_j} \tag{3}$$

$\rho_i$ (mol m$^{-3}$) is the density of the i-th gas at the recorded temperature, and $C_i$ (mg L$^{-1}$) is the i-th gas concentration during the sampling period; $Q_{gas, j}$ (L min$^{-1}$) is the gas flow rate emitted from the j-th tank; $A_j$ (m$^2$) represents the emitted surface of the j-th tank.

## 2.5. N$_2$O-N emission factors

For each compartment, the evaluation of the N$_2$O-N emission factors, expressed as the percentage of N$_2$O-N emitted compared to the inlet nitrogen loading rates, was conducted by means of the following equation (Tsuneda et al., 2005):

$$EF_{N2O} = \frac{N_2O - N_{Gas}/HRT_{h,s} + N_2O - N_{Dissolved}/HRT}{TN_{IN}/HRT} \quad (4)$$

where $EF_{N2O}$ is the emission factor, N$_2$O-N$_{Gas}$ [mg N$_2$O-N L$^{-1}$] is the nitrous dioxide in the gaseous phase, N$_2$O-N$_{Dissolved}$ [mg N$_2$O-N L$^{-1}$] is the nitrous dioxide in the liquid phase, TN$_{IN}$ [mg TN L$^{-1}$] is the pilot plant influent total nitrogen concentration, HRT [h] is the hydraulic retention time of the UCT-MBR pilot plant and HRT$_{h,s}$ [h] represents the hydraulic retention time of the headspace of the analysed tank. In details, the HRT$_{h,s}$ resulted on average equal to 6.18, 11.58, 0.06 and 0.02 h for anaerobic, anoxic, aerobic and MBR reactor, respectively.

Furthermore, the N$_2$O-N mass balance inside each tank has been also performed in order to evaluate the amount of produced/consumed N$_2$O-N according to Equation [5].

$$N_2O - N_{p,c} = N_2O - N_{Dissolved,OUT} + N_2O - N_{Gas,OUT} - N_2O$$
$$- N_{Dissolved} \quad (5)$$

where: N$_2$O-N$_{Dissolved,IN}$ [mg N$_2$O-N h$^{-1}$] and N$_2$O-N$_{Dissolved,OUT}$ [mg N$_2$O-N h$^{-1}$] are fluxes of dissolved N$_2$O-N, entering and exiting a reactor, respectively; N$_2$O-N$_{Gas,OUT}$ [mg N$_2$O-N h$^{-1}$] is the gaseous N$_2$O-N exiting a reactor; N$_2$O-N$_{p,c}$ [mg N$_2$O-N h$^{-1}$] is the flux of N$_2$O-N produced (if positive) or consumed (if negative) in the reactor. Considering fluxes reveals where the N$_2$O is produced because N$_2$O could be produced in an unaerated reactor but exit the system by stripping from an aerated reactor.

## 3. Results and discussion

In order to better understand the key factors mainly affecting the N$_2$O emission, results in terms of pilot plant performance and respirometric batch tests will be first discussed below (sections 3.1 and 3.2). Following, results related to the N$_2$O will be presented and discussed (sections 3.3–3.9).

### 3.1. Pilot plant performances

Table 2 summarizes the average values of pollutant removal efficiency for each experimental phase. In terms of organic carbon

**Table 2**
Average values of the pollutants removal efficiencies for each experimental phase.

| Description | Phase I | Phase II |
|---|---|---|
| Total COD removal efficiency ($\eta_{TOT}$) [%] | 98.4 | 98.4 |
| Biological COD removal efficiency ($\eta_{BIO}$) [%] | 82.8 | 73 |
| Nitrification efficiency ($\eta_{nit}$) [%] | 95.6 | 79 |
| Denitrification efficiency ($\eta_{denit}$) [%] | 59 | 26.5 |
| Total nitrogen removal efficiency ($\eta N_{total}$) [%] | 71 | 33.8 |
| Phosphorus removal efficiency ($\eta P$) [%] | 70 | 2 |

removal, during Phase I (C/N = 10 mgCOD/mgTN), a quite high COD removal efficiency was obtained both in terms of biological and total removal (average value of $\eta_{TOT}$ = 98.4%; average value of $\eta_{BIO}$ = 82.8%) (Table 2). A detailed discussion of the pilot plant performance is provided in the literature (Mannina et al., 2016b). Differences were observed in the biological removal efficiency during Phase II (C/N = 5 mgCOD/mgTN). Indeed, despite the lower C/N, the average biological removal contribution decreased to 73% (Table 2). However, during Phase II, the total COD removal remained quite high, with an average value equal to 98.4% (Table 2). This result was mainly due to the membrane retaining effect. Indeed, the membrane is able to retain most of the non-biodegraded particulate COD and a portion of the soluble COD (in the range of 0.04–0.45 μm). Thus, the membrane was able to assure high performance of the system in terms of total COD removal, despite the reduction of the biological process efficiency.

In terms of nitrogen removal, during Phase I (C/N = 10 mgCOD/mgTN), a quite high nitrogen removal efficiency was observed. Indeed, $\eta_{nit}$, $\eta N_{total}$ and $\eta_{denit}$ were equal to 95.6%, 71% and 59%, respectively. However, during Phase II (C/N = 5 mgCOD/mgTN), due to the higher nitrogen loading rate, the nitrification performance decreased compared to Phase I (average $\eta_{nit}$ during Phase II equal to 79%) (Table 2). During both experimental phases, no significant difference of pH values inside the aerobic tank was noticed (7.84 and 7.86 in the Phase I and II as average values, respectively). Consequently, a decrease of both $\eta N_{total}$ and $\eta_{denit}$ occurred during Phase II (33.8% and 26.5%, respectively) (Table 2). Indeed, the lower C/N value (corresponding to a higher TN$_{IN}$ loading rate) might have inhibited the biomass activity, referring in particular to autotrophic species. Indeed, during phase II, high pH values (average value in Phase II equal to 8.1) and ammonium nitrogen concentration (up to 93 mg NH$_4$-N L$^{-1}$) occurred inside the reactors as a consequence of the decrease of C/N ratio. In such conditions, the Free Ammonia (FA) concentration increased in the mixed liquor (up to 4.5 mg NH$_3$-N L$^{-1}$ at the end of the Phase II). The increase of FA value might have caused a stress effect on the growth of nitrifying species. In particular, the nitrite oxidizing bacteria (NOB) species that are known to be more sensitive to FA compared to ammonia oxidizing bacteria (AOB) (Mannina et al., 2016b; Cydzik-Kwiatkowska et al., 2013). Indeed, Anthonisen et al. (1976) suggested that value of FA from 0.1 to 1.0 mg/L inhibit the NOB growth. Therefore, when operating the system at a low C/N value, a decrease of the nitrogen removal efficiency is expected. Indeed, the average NO$_3^-$ concentration in the anoxic tank, during Phase II, was quite high (close to 31 mg/L). Important to precise is that different nitrogen removal results could have been achieved by reducing the C/N ratio through the reduction of influent COD.

In terms of P removal efficiency, it was satisfactory during Phase I, with an average value of 70%. However, the low C/N ratio during Phase II had a significant influence on the system performance in terms of P removal. In particular, a very low removal efficiency was achieved during Phase II (see Table 2). Indeed, during Phase II, the effluent P concentrations increased to 6.2 mg L$^{-1}$ (average value), which was higher than the average influent P concentration (5.4 mg L$^{-1}$), suggesting that there was no net P removal, likely due to the release of the metabolic P. Moreover, the average Redox value in the anaerobic tank during Phase II was not very low (+48 mV) likely due to the high concentrations of nitrates inside the tank. The decrease of the denitrification efficiency in Phase II caused the increase of the NO$_3$-N loading rate recirculated from the anoxic to the anaerobic tank during Phase II. Thus, inside the anaerobic tank, an average NO$_3$-N concentration of 17 mg L$^{-1}$ was measured during Phase II. This value is significantly higher than the threshold concentration (equal to 1 mg NO$_3$-N L$^{-1}$) required to ensure strong PAO activity in the anaerobic tank (Wentzel et al., 1990). Moreover, it is

worth noting that throughout the experimental campaign, it was found that the biological processes inside the MBR tank were almost negligible. The biological performances in terms of COD, N and P removal of each experimental phase have on average influenced the $N_2O$ production/emission as detailed in the following sections. However, no clear correlation was found, confirming the findings of Daelman et al. (2013) which suggest that during the long term analysis a very poor correlation between the influent feature and the plant performance occurred for a Carrousel reactor. Furthermore, regarding to the membrane fouling, by reducing the C/N to 5 a decrease of the membrane filtration properties took place despite the fouling properties remained stable. Averaged value of TMP resulted equal to −0.28 bar and −0.22 bar for Phase I and II respectively, and averaged value of membrane permeability ($K_{20}$) resulted equal to 128.14 L m$^{-2}$ h$^{-1}$ bar$^{-1}$ and 120.66 L m$^{-2}$ h$^{-1}$ bar$^{-1}$ for Phase I and II respectively. For a more detailed discussion regarding the membrane fouling during the experimentation, the reader is addressed to Mannina et al. (2016b).

## 3.2. Biomass respiratory activity

A detailed discussion on the biomass respiratory activity for the case under study, including the value of the main kinetic/stoichiometric parameters both for heterotrophic and autotrophic species, is provide in Mannina et al. (2016b).

The results have highlighted that the C/N ratio variation exerted a significant effect on biomass activity. Indeed, concerning heterotrophic species, significant decreases of the maximum growth rate ($\mu H_{,max}$) and the specific OUR (SOUR) rates were observed. In particular, the SOUR values after sodium acetate addition provided a good indication of heterotroph viability, highlighting a significant difference in biomass activity in the two experimental phases. Concerning the autotrophic species, during Phase I (C/N = 10 mgCOD/mgTN) a high level of nitrification ability was observed. The autotrophic biokinetic/stoichiometric parameters obtained for the Phase I are in good agreement with the technical literature (Henze et al., 1987). Conversely, during Phase II (C/N = 5 mgCOD/mgTN), a significant decrease of the nitrification ability was observed. Such a result might be related to the higher ammonia loading rate and to the high pH and free ammonia that could have stressed the activity of the autotrophic populations. Such a result was also confirmed by the AUR batch test performed with biomass samples withdrawn from the aerobic compartment (Mannina et al., 2016b). Indeed, during Phase I, the biomass showed high nitrification activity with no nitrite accumulation during the test, and an ammonia utilization rate equal to 2.02 mg NH$_4$-N g$^{-1}$ VSS h$^{-1}$. Conversely, during Phase II, a slight decrease of the nitrification ability was observed, with the ammonia utilization rate decreasing to 0.505 mg NH$_4$-N g$^{-1}$ VSS h$^{-1}$. However, it is worth noting that at the end of the experiments, the ammonia utilization rate increased to 1.362 mg NH$_4$-N g$^{-1}$ VSS h$^{-1}$, thus suggesting acclimation of the autotrophic species to the higher N loading rate in the Phase with the lower C/N ratio. If the decrease of C/N would be realized through a COD decrease, maybe the results would have been different. However, such an aspect was out of the scope and deserves further future studies.

The variation of the results in terms of ammonia utilization rate could have affected the $N_2O$ emissions during the two experimental phase. Indeed, previous studies have demonstrated that the NH$_4$-N oxidation rate had a positive correlation with the $N_2O$ production rate, even if it does not affect the $N_2O$ emission factor (Law et al., 2012; Schneider et al., 2013).

Concerning the denitrification activity, the NUR tests showed nitrate utilization rates equal to 3.20 mg NO$_3$-N g$^{-1}$VSS h$^{-1}$. During Phase II, a decrease of the denitrification activity was observed,

with nitrate utilization rates down to 0.299 mg NO$_3$-N g$^{-1}$VSS h$^{-1}$. This result was likely related to the decrease of the inlet carbon source compared to the available nitrogen, leading to the decrease of the denitrification ability and poorer assimilation of organic matter. This behaviour was in good agreement with previous results reported in the technical literature (Fu et al., 2009). Nevertheless, at the end of the experiments, the denitrification ability was restored, with an increase of the nitrate uptake rate, highlighting a sort of acclimation of the heterotrophic biomass to the low C/N ratio. The decrease of the nitrate utilization rate form the Phase I to the Phase II could have affected the $N_2O$ emission during the denitrification. Previous studies have demonstrated that decreasing the C/N ratio the denitrification rate decrease with a consequent increase of the $N_2O$ emission (Wu et al., 2014).

## 3.3. Total plant $N_2O$-N flux versus influent and effluent features

In Fig. 2 the correlations between the total $N_2O$-N flux emitted from the pilot plant (evaluated as the sum related to each tank having a standard deviation, SD, of ±4.46 mg $N_2O$-N m$^{-2}$ h$^{-1}$) and the influent features in terms of NH$_4$-N concentration (SD = ±31.8 mg NH$_4$-N L$^{-1}$) (Fig. 2a) and C/N ratio (SD = ±4.8 mgCOD/mgTN) (Fig. 2b) are reported. Moreover, the correlations between the total $N_2O$-N flux emitted from the pilot plant and effluent characteristics as NO$_2$-N (SD = ±0.18 mg NO$_2$-N L$^{-1}$) (Fig. 2c) and NO$_3$-N concentration (SD = ±19.5 mg NO$_3$-N L$^{-1}$) (Fig. 2c) are also reported in Fig. 2. By analysing Fig. 2 one can observe that, despite a trend can be identified, a very poor coefficient of determination ($R^2$) was found for the analysed correlations. Therefore, none of the investigated wastewater features correlated strongly with the plant's total $N_2O$ emitted flux (Fig. 2a–b). Indeed, as reported in Fig. 2 the highest $R^2$ value which refers to the correlation with the influent NH$_4$-N concentration is equal to 0.44. Such a result contrasts with the literature findings which suggest that a strong correlation exists between the influent nitrogen load and the $N_2O$ emission (Chandran et al., 2011; Lotito et al., 2012). Analogously, no clear correlation was found between the total $N_2O$-N flux and the permeate concentration of NO$_2$-N (Fig. 2c) or NO$_3$-N (Fig. 2d). Even this latter result contrasts with the main literature results which suggest that the $N_2O$-N emissions depend for example on the pick of NO$_2$-N (Lotito et al., 2012). However, literature findings often refer to short-term analysis where a great variability of $N_2O$-N production takes place. Indeed, Daelman et al. (2013) suggest to consider for a short term analysis composite samples in order to capture the $N_2O$-N variability. However, the results obtained by Daelman et al. (2015) corroborate our findings. Indeed, for a long-term sampling campaign Daelman et al. (2015) found a very poor correlation between the total daily $N_2O$-N emission and the influent features.

## 3.4. Gaseous $N_2O$-N concentration and flux

In Fig. 3, the average $N_2O$-N concentration (a) in the gas phase and the correspondent emitted flux (b) are reported for each tank over the entire experimental period (Phase I, C/N = 10 mgCOD/mgTN and Phase II, C/N = 5 mgCOD/mgTN).

The results reported in Fig. 3 clearly highlight the influence of the C/N ratio on $N_2O$-N production. During Phase I (C/N = 10 mgCOD/mgTN), the $N_2O$-N concentration in each tank was lower than during Phase II (C/N = 5 mgCOD/mgTN). The highest concentration measured during Phase I was equal to 55 μg $N_2O$-N L$^{-1}$, which was achieved in the anoxic tank on the 41st experimental day. This result is consistent with previous studies that identified the anoxic reactor as the major contributor to $N_2O$-N production (Kampschreur et al., 2009; Otte et al., 1996). Indeed, $N_2O$ is an

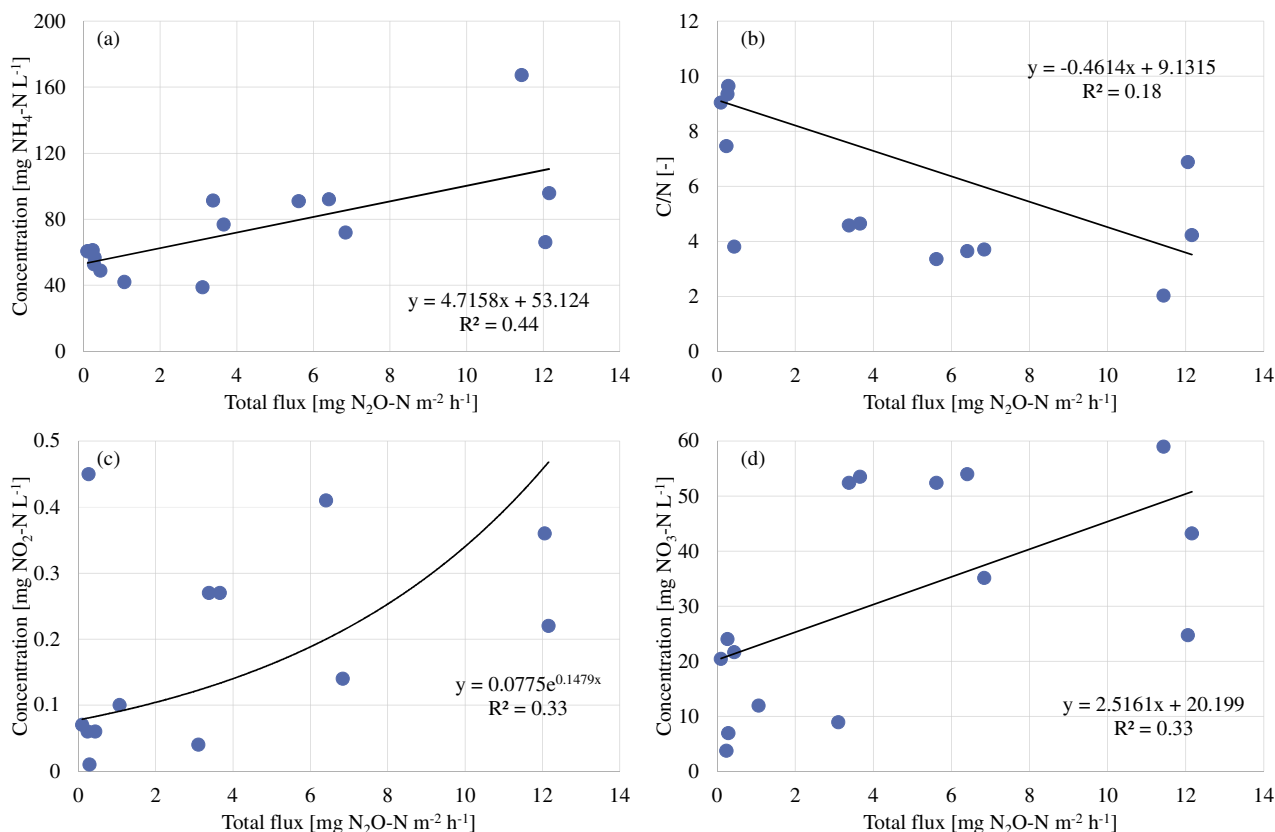**Fig. 2.** Correlation between the total flux emitted from the pilot plant and the influent NH$_4$-N concentration (a), C/N ratio (b), permeate concentration of NO$_2$-N (c) and NO$_3$-N (d).
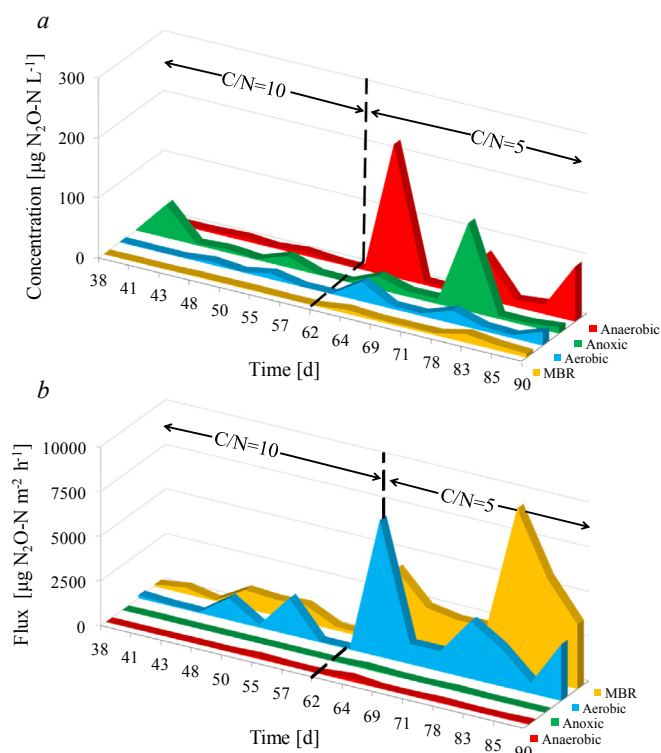


**Fig. 3.** N$_2$O-N concentration in the gas phase (a) and emitted flux (b) for each experimental phase (Phase I, C/N = 10 mgCOD/mgTN and Phase II, C/N = 5 mgCOD/ mgTN).

intermediate product of the NO$_3^-$ denitrification pathway; there-fore, incomplete denitrification can lead to N$_2$O emission (Kampschreur et al., 2009).

During Phase II (C/N = 5 mgCOD/mgTN), as expected, the N$_2$O-N concentration of the gas samples significantly increased. Several authors identified the low C/N value as one of the key factors affecting N$_2$O-N production (Hanaki et al., 1992; Schalk-Otte et al., 2000; Itokawa et al., 2001). Similar results were found in literature despite different influent features, plant scheme and operating conditions have been investigated. More precisely, Alinsafi et al. (2008) found that at low C/N ratio the NO$_2$-N accumulation dur-ing denitrification take place inhibiting the N$_2$O reductase and leading to the N$_2$O formation/emissions. Itokawa et al. (2001) found that at low C/N ratio, the endogenous denitrification takes place thus favouring the N$_2$O emissions.

As reported in Fig. 3a, even the N$_2$O-N concentration inside the anaerobic reactor was influenced by the C/N variation. Indeed, the gas sample withdrawn from the anaerobic tank had average N$_2$O-N concentrations of 3.2 μg N$_2$O-N L$^{-1}$ and 53.6 μg N$_2$O-N L$^{-1}$ during experimental Phase I and II, respectively. This result was mainly due to the partial denitrification that occurred inside the anaerobic tank. As discussed above, anoxic conditions occurred inside the anaerobic tank during Phase II due to the high NO$_3$-N concentra-tion. Moreover, inside the anaerobic tank, the high amount of readily biodegradable COD, available as a result of the feeding wastewater flux according to the pilot plant scheme (Fig. 1), enabled heterotrophic biomass growth. Therefore, both circum-stances (the availability of readily biodegradable COD and the high NO$_3$-N concentration) made the environment inside the anaerobic tank adequate for denitrification of the recycled NO$_3$-N.

Despite the lower N$_2$O-N concentrations, the aerated tanks

(aerobic and MBR) provided the highest $N_2O$-N emitted flux (Phase I: 520 µg $N_2O$-N $m^{-2}$ $h^{-1}$ and 539 µg $N_2O$-N $m^{-2}$ $h^{-1}$ for the MBR and aerobic tank, respectively; Phase II: 2390 µg $N_2O$-N $m^{-2}$ $h^{-1}$ and 3764 µg $N_2O$- N $m^{-2}$ $h^{-1}$ for the MBR and aerobic tank, respectively) (Fig. 3b). Conversely, the $N_2O$-N flux emitted from the anaerobic and anoxic compartments was negligible throughout the experiments (Phase I: 5 µg $N_2O$-N $m^{-2}$ $h^{-1}$ and 15 µg $N_2O$-N $m^{-2}$ $h^{-1}$ for the anoxic and anaerobic tank, respectively; Phase II: 22 µg $N_2O$-N $m^{-2}$ $h^{-1}$ and 41 µg $N_2O$-N $m^{-2}$ $h^{-1}$ for the anoxic and anaerobic tank, respectively).

Since literature identified BNR processes as the key source of $N_2O$ emissions (Kampschreur et al., 2009; Law et al., 2012; Zhao et al., 2014), the results obtained here (concerning the high $N_2O$ emission in MBR tank) seems to be contrasting with the very low HRT (~0.36 h) of the MBR tank. Nevertheless, despite at this low HRT value the occurrence of biological processes can be considered negligible (referring in particular to nitrification), it is not possible to exclude a further production of $N_2O$, also considering that its concentration is at least one order of magnitude smaller compared to ammonium. Moreover, the high $N_2O$-N fluxes from the MBR tank are mostly related to the high $N_2O$-N produced inside the aerobic reactor. Indeed, a great amount of the dissolved $N_2O$ produced inside the aerobic tank is pumped from the aerobic to the MBR tank through $Q_{RAS}$. Therefore, the MBR becomes a great source of the $N_2O$ flux as a result of the stripping effect applied by the aeration system for fouling mitigation. The $N_2O$-N in the water phase produced in the aerobic reactor is then transformed to the gas phase and emitted in the MBR. Therefore, the processes occurring inside the aerobic tank were crucial in terms of $N_2O$-N flux emission. Indeed, as suggested by the technical literature, AOB bacteria are capable of producing $N_2O$ during ammonia oxidation (Kampschreur et al., 2008). Furthermore, AOB denitrification is believed to be the main $N_2O$-N production pathway in biological wastewater treatment under aerobic conditions (Wunderlin et al., 2012; Colliver and Stephenson, 2000).
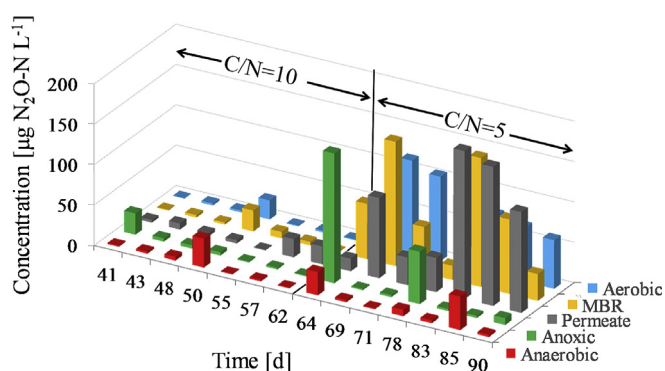


**Fig. 4.** Nitrous oxide concentrations in the liquid phase.

### 3.5. Dissolved $N_2O$-N concentration

In Fig. 4, the average $N_2O$-N dissolved concentrations for each sampling day are reported.

The achieved results confirmed the data related to the gaseous phase in terms of relation between low C/N and increased $N_2O$ production process. In detail, the average concentrations measured during both experimental phases are summarized in Table 3. Data reported in Table 3 have the same order of magnitude of the results achieved in other studies in literature. For example, Pan et al. (2016) in a plug-flow activated sludge reactor found that for different step-feed configurations the amount of dissolved $N_2O$-N varies in the range of 0–0.48 mgN $L^{-1}$.

Data reported in Table 3 highlight that from Phase I through Phase II, the $N_2O$ production was higher with a lower C/N ratio, as previously discussed for the gaseous form. Such a result represents an indirect effect of the low C/N (due to the increase of pH and FA) on the $N_2O$ production. Data reported in Table 3 show that the dissolved $N_2O$-N average concentrations during Phase II were higher (an order of magnitude, except in the anaerobic reactor) than during Phase I. This result could likely be due to the lower nitrification occurred during the Phase II. Indeed, as discussed in Mannina et al. (2016b)during the Phase II an increase of the FA occurred inside the aerobic tank (up to 4.5 mg $NH_3$-N $L^{-1}$ at the end of the Phase II) which would have limited the growth of nitrifying species. The $N_2O$-N concentrations measured in the aerobic and MBR compartments were higher than those in the anoxic and anaerobic compartments, in accordance with the results achieved in terms of $N_2O$-N fluxes. The higher N-loading rate could be the reason for the higher $N_2O$-N emission.

The results indicate that a quite high concentrations of $N_2O$-N were measured in the permeate flow. Indeed, the dissolved $N_2O$-N concentration in the permeate was significantly higher than in the MBR suggesting a significant role of the biofilm formed on the membrane surface (cake layer) in nitrous oxide emission. Nevertheless, the rate of biofilm contribution was not measured and requires in-depth measure not carried out in this study.

The relevant $N_2O$-N in the permeate differ from previous study assumptions where the presence of nitrous oxide in the effluent is considered a negligible fraction of the whole gas present in the WWTPs (Guo et al., 2012). Specifically, $N_2O$-N discharged with effluent flow represents the 0.01% and the 0.1% of the total influent nitrogen for the Phase I and Phase II, respectively. Despite the percentage reported above seems to be negligible, one has to consider that the dissolved $N_2O$ discharged with the effluent flow can be emitted in the atmosphere in gaseous form with a very high GWP (298 times higher than $CO_2$).

Moreover, the experimental results demonstrated that the $N_2O$-N in the water phase discharged to the receiving water body might be higher than that emitted in the gas phase from the WWTP (16.1 mg $N_2O$-N/day as gaseous emission and 25.6 mg $N_2O$-N/day as

**Table 3**
Minimum, average, maximum and standard deviation (SD) values of the dissolved $N_2O$-N concentrations measured during both experimental phases.

| Phase | | Anoxic | Anaerobic | Aerobic | MBR | Permeate |
|---|---|---|---|---|---|---|
| | | [µg $N_2O$-N $L^{-1}$] | [µg $N_2O$-N $L^{-1}$] | [µg $N_2O$-N $L^{-1}$] | [µg $N_2O$-N $L^{-1}$] | [µg $N_2O$-N $L^{-1}$] |
| I | Min | 0.62 | 0.59 | 0.32 | 0.56 | 0.53 |
| | Mean | 3.88 | 4.39 | 3 | 4.17 | 5.86 |
| | Max | 16.73 | 22.76 | 14.98 | 16.48 | 14.37 |
| | SD (±) | 5.73 | 8.14 | 5.30 | 5.64 | 5.84 |
| II | Min | 1 | 0.8 | 22.7 | 11.1 | 9.8 |
| | Mean | 20.9 | 7.8 | 42.7 | 49.6 | 57.5 |
| | Max | 102.3 | 26.3 | 73.6 | 101.6 | 116.5 |
| | SD (±) | 14.63 | 9.03 | 19.67 | 36.77 | 39.12 |

liquid emission with the effluent). Such a result suggests that serious attention must be paid to the effluent quality of the WWTP also in terms of dissolved $N_2O$-N. Since the $N_2O$ will be stripped inside the receiving water body, an uncontrolled discharge could be very harmful to the quality of the atmosphere around the discharge point.

### 3.6. $N_2O$-N mass balance over the tanks

For sake of completeness in Fig. 5 the $N_2O$-N mass balance over the tanks is reported. By analysing Fig. 5 one may observe that during Phase I $N_2O$-N production/consumption occurred inside the pilot plant (Fig. 5a). Conversely, during Phase II inside the aerobic, anoxic and MBR a great amount of $N_2O$-N was produced or consumed (Fig. 5b–c). More precisely, inside the anoxic tank $N_2O$-N has been mostly consumed with an average value of 0.83 mg $N_2O$-N $h^{-1}$ (Phase II) (Fig. 5b). Important to precise is that, the measured $N_2O$ consumption in the ODR was negligible (namely, less than 1%).
.

### 3.7. $N_2O$-N emission factors

Fig. 6 shows the $N_2O$-N emission factors of each compartment, expressed as a percentage of the total nitrogen load of the plant (see Equation (4)) throughout the experiments. Based on Fig. 6, it is worth noting that the EF increases with the decrease of the C/N value. Indeed, the total EF, expressed as the sum of the EF of each compartment, is equal to 3.82% and 10.26% (as average) for Phase I and II, respectively (Fig. 7). This result is consistent with previous literature data that suggest the increase of EF with the decrease of
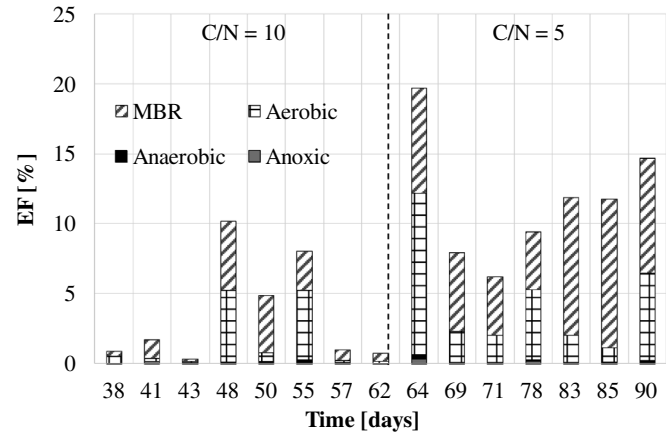


**Fig. 6.** $N_2O$-N emission factor pattern for during experiments (Phase I: C/N = 10 mgCOD/mgTN; Phase II: C/N = 5 mgCOD/mgTN).

C/N (Hanaki et al., 1992; Itokawa et al., 2001). Moreover, previous studies on a full scale conventional AS-UCT plant (i.e. without membrane filtration units) showed that the EF values were in line (slight lower) to what observed in the present study, for similar operating conditions (domestic wastewater, C/N = 9 and HRT = 19 h) (Sperandio et al., 2016). Furthermore, the EF of the anaerobic and anoxic reactors can be neglected (Fig. 7a). The high total EF value (on average) during Phase II is most likely due to the significant decrease of the system nitrification ability, as confirmed by the respirometric batch test results. The greatest EF contribution derives from the two aerated reactors (namely, the aerobic and
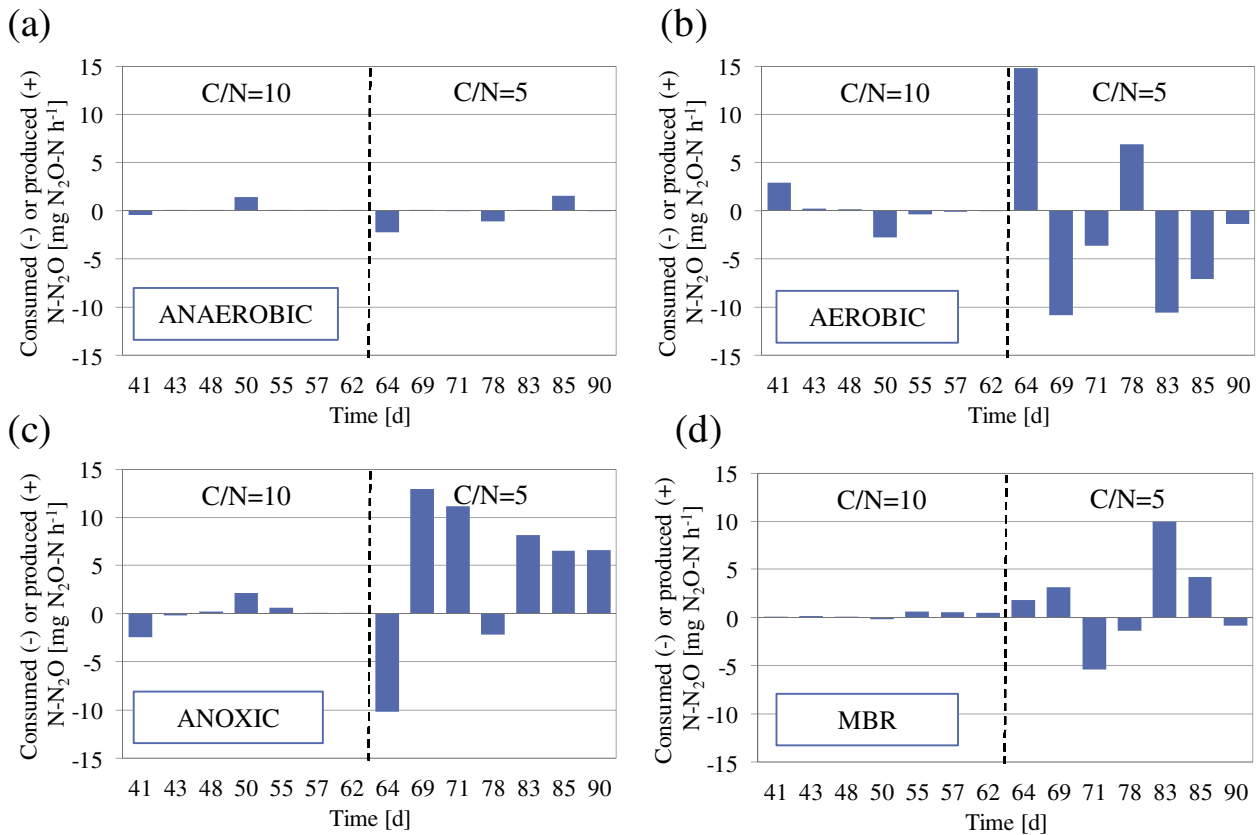


**Fig. 5.** $N_2O$-N mass balance for the anaerobic (a), anoxic (b), aerobic (c) and MBR (d) tank for each experimental phase (Phase I, C/N = 10 mgCOD/mgTN and Phase II, C/N = 5 mgCOD/mgTN).
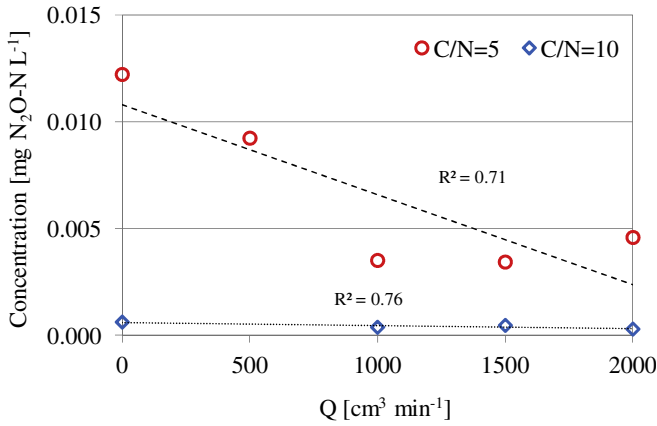
**Fig. 7.** N$_2$O-N concentration at different Q$_{sweep}$ for each experimental phase (Phase I: C/N = 10; Phase II: C/N = 5) in the samples withdrawn from the anoxic tank.

MBR reactors). The inhibition of the nitrification process inside the aerobic reactor is responsible for the production of N$_2$O-N, either dissolved or gaseous. A fraction of the dissolved N$_2$O-N is emitted

due to the aeration from the aerobic tank. Since a great amount of dissolved N$_2$O-N load is pumped from the aerobic tank to the MBR tank, it is also emitted from the MBR tank due to the intensive aeration (fouling mitigation).

### 3.8. The influence of the sweep air-flow rate

During the two experimental phases, the role of sweep air on the N$_2$O-N concentration measured in the headspace of the anoxic zone was investigated. As discussed in the literature, the mixing caused by the sweep air ensures the collection of a representative gas concentration (Chandran et al., 2011). More precisely, during the two experimental phases, an ad-hoc campaign was performed by promoting gas mixing inside the anoxic headspace at different sweep air flow rates (Q$_{sweep}$). The gas sampling frequency was set on the basis of the time required for the saturation of the headspace volume.

Fig. 7 shows the results of the N$_2$O-N concentration for each experimental phase (Phase I: C/N = 10 mgCOD/mgTN; Phase II: C/N = 5 mgCOD/mgTN), measured at different Q$_{sweep}$ values in the gas samples withdrawn from the anoxic tank.
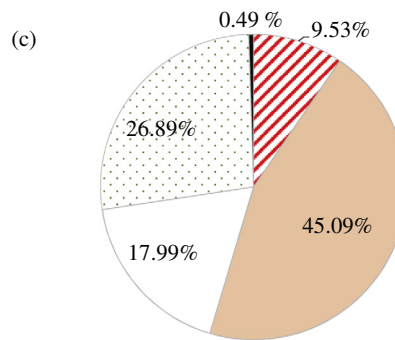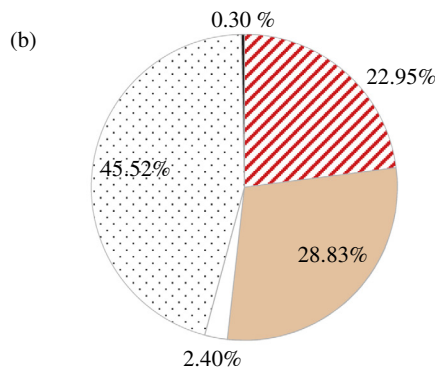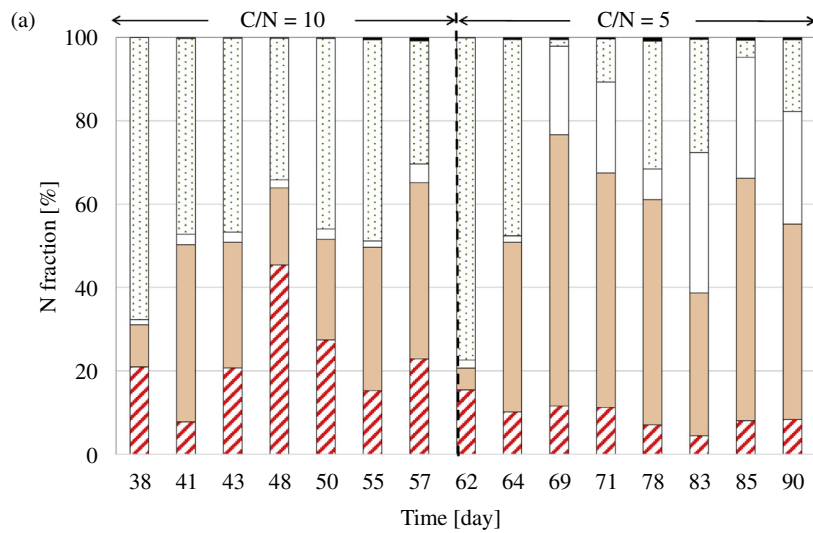


**Fig. 8.** Trend of nitrogen forms expressed as a percentage of the total influent nitrogen throughout experiments (a); percentage of each nitrogen form (as average) referring to the Phase I (b) and the Phase II (c), respectively.

By analysing Fig. 7, one can observe that the N$_2$O-N concentration (on average) was one order of magnitude higher when the C/N ratio was reduced to 5, equal to 0.44 and 5.2 μg N$_2$O-N L$^{-1}$ for C/N ratios of 10 mgCOD/mgTN and 5 mgCOD/mgTN, respectively (Fig. 7).

Such differences confirm the negative impact exerted by the low C/N ratio on N$_2$O-N production. Indeed, several studies report similar results; for example, Itokawa et al. (2001) found that when the C/N ratio was below 3.5, the nitrous oxide emitted was up to 20–30% of the nitrogen load.

Furthermore, it is worth noting that in both phases, the sweep air variation induced the same dilution effect on the N$_2$O-N concentration. For both phases, the N$_2$O-N concentration at a Q$_{sweep}$ of 1000 cm$^3$ min$^{-1}$ was approximately 30% of that at a Q$_{sweep}$ equal to zero. For a Q$_{sweep}$ higher than 1000 cm$^3$ min$^{-1}$, the N$_2$O-N concentration remained almost stable (Fig. 7). Therefore, in the present study, a Q$_{sweep}$ equal to 1000 cm$^3$ min$^{-1}$ can be considered as a threshold value, beyond which complete gas mixing inside the anoxic headspace occurs.

### 3.9. Nitrogen mass balance

Fig. 8 shows the mass balance of the nitrogen forms throughout the experimental campaign (Fig. 8a) and the average values of each N fraction for both experimental phases (Fig. 8b and c, respectively, Phase I and Phase II).

Important to precise is that the data reported in Fig. 8 show how the influent N has been transformed inside the pilot plant and the forms in which N has been discharged into the environment (in gaseous or dissolved forms).

By analysing Fig. 8, one can observe that the influent C/N ratio variation from 10 mgCOD/mgTN (Phase I) to 5 mgCOD/mgTN (Phase II) strongly influenced the N transformation inside the pilot plant. More precisely, during Phase I, a great amount of influent nitrogen was metabolized by the biomass (approximately 23% on average, Fig. 8a–b), thus confirming the high biomass activity during Phase I. Conversely, during Phase II, the amount of metabolic N was reduced to 9.53% (on average) due to a reduction of the biomass activity (Fig. 8a–c). The reduced autotrophic biomass activity during Phase II led to the increase of the effluent NH$_4$-N fraction from 2.4% (Phase I) to 17.99% (Phase II). On the other hand, the reduced heterotrophic activity during Phase II caused the increase of the effluent NO$_3$-N fraction from 28.83% (Phase I) to 45.09% (Phase II) and, consequently, a decrease of the denitrified N fraction from 45.52% (Phase I) to 26.89% (Phase II) (Fig. 8a–c). Furthermore, the increase of the average effluent N$_2$O-N percentage (both gaseous and dissolved) occurred from Phase I (effluent N$_2$O-N gas = 0.03%; effluent N$_2$O-N dissolved = 0.03%) (Fig. 8b) through Phase II (effluent N$_2$O-N gas = 0.1%; effluent N$_2$O-N dissolved = 0.09%) (Fig. 8c).

## 4. Conclusions

In this study it was presented the first study on the overall assessment of N$_2$O emissions from a fully covered UCT-MBR pilot plant distinguishing the contributions of the different tanks and quantifying the stripping effect due to aeration for membrane fouling mitigation. Furthermore, the effect of C/N variation on N$_2$O-N emissions from a UCT-MBR pilot plant was investigated. The following conclusions can be drawn:

- The study confirms that in the BNR systems (including MBR) the nitrification is the major source of N$_2$O-N in terms of emitted flux.

- Denitrification process represents an effective sink of N$_2$O; indeed, even at low C/N (Phase II), a net value of 0.83 mg N$_2$O-N h$^{-1}$ were consumed inside the anoxic tank.
- The high aeration for fouling mitigation inside the membrane tank strongly contributes to the increase of the N$_2$O-N in the gas phase due to the stripping effect; such a result suggests a sort of warming when MBR are operated: do not neglect the contribution of the membrane tank during the evaluation of the total amount of the N$_2$O emission.
- The highest dissolved N$_2$O-N concentration observed in the permeate flow suggests that processes likely occurred inside the cake layer can contribute to the N$_2$O production; further investigations in terms of nitrification or denitrification rate inside the cake layer are required for the future to confirm this statement. This result emphasizes the need to pay in the future more attention also on N$_2$O-N emissions to protect the receiving water bodies.
- The EF values highlighted that most of the emissions derived from the membrane compartment, mainly due to the stripping effect exerted by the intensive aeration.
- The low C/N ratio (namely, 5) in BNR systems causes the increase of both pH and free ammonia thus promoting the N$_2$O emission caused by their inhibition effect on autotrophic biomass. Therefore, this study confirms that the C/N represents an indirect operating factor influencing the N$_2$O emission.

## References

Alinsafi, A., Adouani, N., Béline, F., Lendormi, T., Limousy, L., Sire, O., 2008. Nitrite effect on nitrous oxide emission from denitrifying activated sludge. Process Biochem. 43, 683–689.

Anthonisen, A.C., Loehr, R.C., Prakasam, T.B.S., Srinath, E.G., 1976. Inhibition of nitrification by ammonia and nitrous acid. J. Water Pollut. Control Fed. 48, 835–852.

APHA, 2005. Standard Methods for the Examination of Water and Wastewater. APHA, AWWA and WPCF, Washington DC, USA.

Chandran, K., Stein, L.Y., Klotz, M.G., van Loosdrecht, M.C.M., 2011. Nitrous oxide production by lithotrophic ammonia oxidizing bacteria and implications for engineered nitrogen-removal systems. Biochem. Soc. Trans. 39, 1832–1837.

Colliver, B.B., Stephenson, T., 2000. Production of nitrogen oxide and dinitrogen oxide by autotrophic nitrifiers. Biotechnol. Adv. 18 (3), 219–232.

Cydzik-Kwiatkowska, A., Zielińska, K., Bernat, M., Wojnowska-Baryła, I., Truchan, T., 2013. Treatment of high-ammonium anaerobic digester supernatant by aerobic granular sludge and ultrafiltration processes. Chemosphere 90, 2208–2215.

Daelman, M.R.J., De Baets, B., Volcke, E.I.P., van Loosdrecht, M.C.M., 2013. Influence of sampling strategies on the estimated nitrous oxide emission from wastewater treatment plants. Water Res. 47, 3120–3130.

Daelman, M.R.J., van Voorthuizen, E.M., van Dongen, U.G.J.M., Volcke, E.I.P., van Loosdrecht, M.C.M., 2015. Seasonal and diurnal variability of N$_2$O emissions from a full-scale municipal wastewater treatment plant. Sci. Total Environ. 536, 1–11.

Frison, N., Chiumenti, A., Katsou, E., Malamis, S., Bolzonella, D., Fatone, F., 2015. Mitigating off-gas emissions in the biological nitrogen removal via nitrite process treating anaerobic effluents. J. Clean. Prod. 93, 126–133.

Fu, Z., Yang, F., Zhou, F., Xue, Y., 2009. Control of COD/N ratio for nutrient removal in a modified membrane bioreactor (MBR) treating high strength wastewater. Bioresour. Technol. 100, 136–141.

Guo, L., Porro, J., Sharma, K.R., Amerlinck, Y., Benedetti, L., Nopens, I., Shaw, A., Van Hulle, S.W.H., Yuan, Z., Vanrolleghem, P.A., 2012. Towards a benchmarking tool for minimizing wastewater utility greenhouse gas footprints. Water Sci.

Technol. 66 (11), 2483–2495.

Hanaki, K., Hong, Z., Matsuo, T., 1992. Production of nitrous oxide gas during denitrification of wastewater. Water Sci. Technol. 26 (5–6), 1027–1036.

Henze, M., Grady Jr., C.P.L., Gujer, W., Marais, G.V.R., Matsuo, T., 1987. Activated Sludge Model No.1, IAWPRC Scientific and Technical Report No.1. IAWPRC, London.

IPCC, 2007. Changes in atmospheric constituents and in radiative forcing. In: Solomon, S., et al. (Eds.), Climate Change 2007: the Physical Science Basis. Contribution of Working Group I to the Fourth Assessment Report of the Intergovernmental Panel on Climate Change. Cambridge University Press, Cambridge, pp. 114–143.

Itokawa, H., Hanaki, K., Matsuo, T., 2001. Nitrous oxide production in high-loading biological nitrogen removal process under low COD/N ratio condition. Water Res. 35 (3), 657–664.

Judd, S.J., Judd, C., 2010. Principles and Applications of Membrane Bioreactors in Water and Wastewater Treatment, second ed. Elsevier, London, UK.

Kampschreur, M.J., Temmink, H., Kleerebezem, R., Jetten, M.S.M., van Loosdrecht, M.C.M., 2009. Nitrous oxide emission during wastewater treatment. Water Res. 43, 4093–4103.

Kampschreur, M.J., van der Star, W., Wielders, H.A., Mulder, J.W., Jetten, M.S.M., van Loosdrecht, M.C.M., 2008. Dynamics of nitric oxide and nitrous oxide emission during full-scale reject water treatment. Water Res. 42, 812–826.

Kimochi, Y., Inamori, Y., Mizuochi, M., Xu, K.-Q., Matsumura, M., 1998. Nitrogen removal and N$_2$O emission in a full-scale domestic wastewater treatment plant with intermittent aeration. J. Ferment. Bioeng. 86, 202–206.

Law, Y., Ye, L., Pan, Y., Yuan, Z., 2012. Nitrous oxide emissions from wastewater treatment processes. Philos. Trans. R. Soc. Lond. B Biol. Sci. 367, 1265–1277.

Li, C., Wang, T., Zheng, N., Zhang, J., Ngo, H.H., Guo, W., Liang, S., 2013. Influence of organic shock loads on the production of N$_2$O in denitrifying phosphorus removal process. Bioresour. Technol. 141, 160–166.

Lotito, A.M., Wunderlin, P., Joss, A., Kipf, M., Siegrist, H., 2012. Nitrous oxide emissions from the oxidation tank of a pilot activated sludge plant. Water Res. 46, 3563–3573.

Mannina, G., Capodici, M., Cosenza, A., Di Trapani, D., 2016b. Carbon and nutrient biological removal in a University of Cape Town membrane bioreactor: analysis of a pilot plant operated under two different C/N ratios. Chem. Eng. J. 296, 289–299.

Mannina, G., Cosenza, A., Di Trapani, D., Laudicina, V.A., Morici, C., Ødegaard, H., 2016d. Nitrous oxide emissions in a membrane bioreactor treating saline wastewater contaminated by hydrocarbons. Bioresour. Technol. 219, 289–297.

Mannina, G., Ekama, G., Caniani, D., Cosenza, A., Esposito, G., Gori, R., Garrido-Baserba, M., Rosso, D., Olsson, G., 2016a. Greenhouse gases from wastewater treatment — a review of modelling tools. Sci. Total Environ. 551–552, 254–270.

Mannina, G., Morici, C., Cosenza, A., Di Trapani, D., Ødegaard, H., 2016c. Greenhouse gases from sequential batch membrane bioreactors: a pilot plant case study. Biochem. Eng. J. 112, 114–122.

Nuansawan, N., Boonnorat, J., Chiemchaisri, W., Chiemchaisri, C., 2016. Effect of hydraulic retention time and sludge recirculation on greenhouse gas emission and related microbial communities in two-stage membrane bioreactor treating solid waste leachate. Bioresour. Technol. 210, 35–42.

Otte, S., Grobben, N.G., Robertson, L.A., Jetten, M.S.M., Kuenen, J.G., 1996. Nitrous oxide production by Alcaligenes faecalis under transient and dynamic aerobic and anaerobic conditions. Appl. Environ. Microb. 62 (7), 2421–2426.

Pan, Y., van den Akker, B., Ye, L., Ni, B.-J., Watts, S., Reid, K., Yuan, Z., 2016. Unravelling the spatial variation of nitrous oxide emissions from a step-feed pulg-flow full scale wastewater treatment plant. Sci. Rep. 6, 20792. http://dx.doi.org/10.1038/srep20792.

Papa, M., Alfonsín, C., Moreira, M.T., Bertanza, G., 2016. Ranking wastewater treatment trains based on their impacts and benefits on human health: a "Biological Assay and Disease" approach. J. Clean. Prod. 113, 311–317.

Quan, X., Zhang, M., Lawlor, P.G., Yang, Z., Zhan, X., 2012. Nitrous oxide emission and nutrient removal in aerobic granular sludge sequencing batch reactors. Water Res. 46, 4981–4990.

Schalk-Otte, S., Seviour, R.J., Kuenen, J.G., Jetten, M.S.M., 2000. Nitrous oxide (N$_2$O) production by Alcaligenes faecalis during feast and famine regimes. Water Res. 34 (7), 2080–2088.

Schneider, Y., Beier, M., Rosenwinkel, K.H., 2013. Nitrous oxide formation during nitritation and nitrification of high-strength wastewater. Water Sci. Technol. 67, 2494–2502.

Sperandio, M., Pocquet, M., Guo, L., Ni, B.-J., Vanrolleghem, P.A., Yuan, Z., 2016. Evaluation of different nitrous oxide production models with four continuous long-term wastewater treatment process data series. Bioprocess Biosyst. Eng. 39 (3), 493–510.

Stenström, F., Tjus, K., la Cour Jansen, J., 2014. Oxygen-induced dynamics of nitrous oxide in water and off-gas during the treatment of digester supernatant. Water Sci. Technol. 69, 84–91.

Tsuneda, S., Mikami, M., Kimochi, Y., 2005. Effect of salinity on nitrous oxide emission in the biological nitrogen removal process for industrial wastewater. J. Hazard Mater 119, 93–98.

Wagner, J., Guimarães, L.B., Akaboci, T.R.V., Costa, R.H.R., 2015. Aerobic granular sludge technology and nitrogen removal for domestic wastewater treatment. Water Sci. Technol. 71 (7), 1040–1046.

Wentzel, M.C., Dold, P.L., Ekama, G.A., Marais, G.R., 1990. Biological excess phosphorous removal-steady state process design. Water SA 16 (1), 29–48.

Wu, G., Zheng, D., Xing, L., 2014. Nitritation and N$_2$O emission in a denitrification and nitrification two-sludge system treating high ammonium containing wastewater. Water 6, 2978–2992.

Wunderlin, P., Mohn, J., Joss, A., Emmenegger, L., Siegrist, H., 2012. Mechanisms of N$_2$O production in biological wastewater treatment under nitrifying and denitrifying conditions. Water Res. 46 (4), 1027–1037.

Yan, X., Li, L., Liu, J., 2014. Characteristics of greenhouse gas emission in three full-scale wastewater treatment processes. J. Environ. Sci. 26, 256–263.

Zhao, W., Wang, Y., Lin, X., Zhou, D., Pan, M., Yang, J., 2014. Identification of the salinity effect on N$_2$O production pathway during nitrification: using stepwise inhibition and 15N isotope labeling methods. Chem. Eng. J. 253, 418–426.